Attitude Determination GPS/INS Integrated Navigation System with FDI Algorithm for a UAV

Sang Heon Oh
Navicom R&D Center, National Co., Ltd.
100 Sinseong-dong, Yuseong-gu, Daejeon 305-345, Korea
Dong-Hwan Hwang*
GNSS Technology Research Center, School of Electrical and Computer Engineering, Chungnam National University, 220 Gung-dong, Yuseong-gu, Daejeon 305-764, Korea
Chansik Park
School of Electrical and Electronics Engineering, Chungbuk National University, 12, Gaeshin-dong, Heungduk-gu, Cheongju 361-763, Korea
Sang Jeong Lee
GNSS Technology Research Center, School of Electrical and Computer Engineering, Chungnam National University, 220 Gung-dong, Yuseong-gu, Daejeon 305-764, Korea
Se Hwan Kim
Navicom R&D Center, Navicom Co., Ltd., 100 Sinseong-dong, Yuseong-gu, Daejeon 305-345, Korea

Recently an unmanned aerial vehicle (UAV) has been widely used for military and civil applications. The role of a navigation system in the UAV is to provide navigation data to the flight control computer (FCC) for guidance and control. Since performance of the FCC is highly reliant on the navigation data, a fault in the navigation system may lead to a disastrous failure of the whole UAV. Therefore, the navigation system should possess a fault detection and isolation (FDI) algorithm. This paper proposes an attitude determination GPS/INS integrated navigation system with an FDI algorithm for a UAV. Hardware for the proposed navigation system has been developed. The developed hardware comprises a commercial inertial measurement unit (IMU) and the integrated navigation package (INP) which includes an attitude determination GPS (ADGPS) receiver and a navigation computer unit (NCU). The navigation algorithm was implemented in a real-time operating system with a multi-tasking structure. To evaluate performance of the proposed navigation system, a flight test has been performed using a small aircraft. The test results show that the proposed navigation system can give accurate navigation results even in a high dynamic environment.

Key Words: Flight Test, GPS, INS, GPS/INS Integration System, Kalman Eilter, Integrity, Fault Detection, UAV

* Corresponding Author,
E-mail: dhhwang@cnu ac.kr
TEL: +82-42-821-5670; **FAX**: +82-42-823-5436
GNSS Technology Research Center, School of Electrical and Computer Engineering, Chungnam National University, 220 Gung-dong, Yuseong-gu, Daejeon 305-764, Korea. (Manuscript **Received** September 29, 2003; **Revised** June 17, 2005)

Nomenclature

$\mathbf{H}_k$: Measurement matrix at time t_k
l_k : Test statistic at time t_k
N : Window size
$N(\mu, \sigma^2)$: Normal distribution with mean μ and variance σ^2
p : Dimension of the residual vector γ_k

$\mathbf{P}_k$: Error covariance matrix at time t_k
$\mathbf{Q}_k$: Covariance matrix of the process noise at time t_k
$\mathbf{R}_k$: Covariance matrix of the measurement noise at time t_k
$\mathbf{V}_k$: Covariance matrix of the residual vector γ_k at time t_k
$\mathbf{x}_k$: State vector at time t_k
$\mathbf{z}_k$: Measurement vector at time t_k
χ^2_n : Chi-square distribution with n degree-of-freedom
ϵ : Decision threshold
γ_k: Residual vector at time t_k

1. Introduction

In recent years, many research activities on the unmanned aerial vehicle (UAV) have been reported and many countries have made efforts to develop the UAV due to its significance in military and civil applications (Tsach et al., 2002). Korea Aerospace Research Institute (KARI) and Agency for Defense Development (ADD) of Korea have been conducting researches in order to develop a UAV. Figure 1 shows an example of a developing UAV in Korea. In Fig. 1, the autopilot system is responsible for the guidance and control of the UAV. The ground control station monitors and manages operation of the UAV and transmits remote commands to the UAV. The navigation system provides navigation data to the flight control computer (FCC) of the autopilot system (Blakelock, 1991 ; Michael, 1988).

The inertial navigation system (INS) provides an accurate navigation solution in short term and has low frequency error that grows with time. The global positioning system (GPS) provides noisy data with long-term accuracy (Grewal et al., 2001). Since the INS and the GPS have complementary features mentioned above, the GPS/

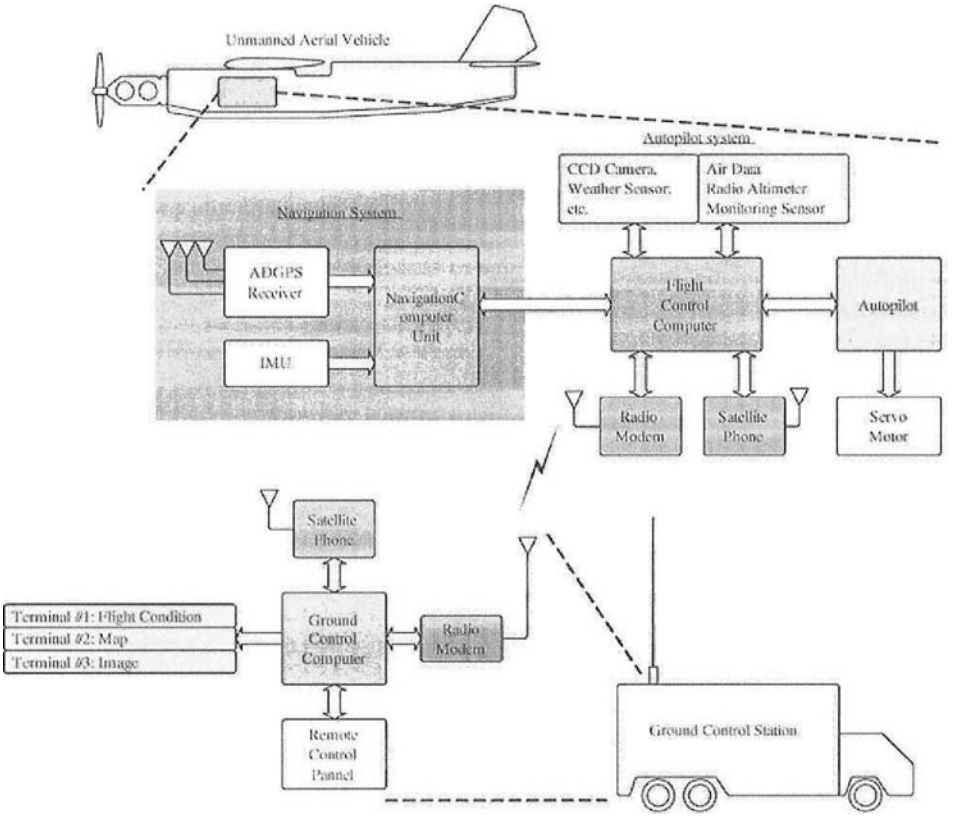

Fig. 1 Autopilot and ground control system for a UAV

INS integration system has been widely used for a main navigation system of various military and commercial vehicles (Cox, 1980). Military applications such as a fighter, a bomber, and a large scale UAV have adopted a highly accurate navigation grade inertial measurement units (IMU) (<0.01 deg/h gyro bias), have been adopted for their GPS/INS integrated navigation system. The navigation system can provide accurate navigation results with high reliability even in high dynamic environment. However, it is relatively expensive, large size, and can be accessible by only restrict users.

On the other hand, GPS/low grade IMU integration systems can be widely utilized for civil applications due to their small size, low cost, and no restriction of use. However, they provide low navigation performance during the coasting or high maneuvering compared to the military GPS/INS integration systems (Gautier and Parkinson, 2003; Rios and White, 2001). Since performance of the GPS/low grade IMU integration system is reliant on the GPS data accuracy, GPS measurement is more weighted than the INS error model in the integrated Kalman filter (Maybeck, 1979). In recent years, an attitude determination GPS (ADGPS) has been used to improve the performance of the GPS/low grade IMU integration system (Gebre-Egziabher et al., 1998; Hong et al., 2002; McMillan, 1994; Satz et al., 1991; Wolf et al., 1996).

Faults in GPS can be caused by failures of a GPS receiver or a malign environment. The GPS receiver can give anomalous outputs due to jamming, multipath, and signal outage. If the Kalman filter in the GPS/INS integration system is not designed to reject these anomalous GPS data, the accuracy of the navigation system can be seriously degraded (Grewal et al., 2001). Since the performance of the autopilot system in the UAV is highly reliant on the navigation data, the fault in the (AD)GPS/INS integrated navigation system may lead to a disastrous failure (Brenner, 1995; Diesel and King, 1995; Sukkarieh et al., 1999). For this reason, the GPS/INS and/or ADGPS/INS integrated navigation system has to possess a fault detection and isolation (FDI) function to cope with the influence of anomalous (AD)GPS data.

This paper proposes an ADGPS/INS integrated navigation system with an FDI algorithm for a UAV. The proposed integration system uses the ADGPS receiver in order to improve the performance of the navigation system even when the low grade IMU is utilized. The FDI algorithm is included to provide a reliable navigation data. In order to verify the effectiveness of the proposed navigation system, a real-time hardware, and software have been developed and a flight test has been performed using a small aircraft. A commercial tactical and automotive grade IMUs has been used for the flight test. The proposed navigation system has been developed under the project, "Development of Autopilot and Ground Control System for a UAV," one of the projects in the Dual Use Technology Research Program (Korea).

This paper is organized as follow; sec. 2 describes the FDI algorithm for the ADGPS/INS integrated navigation system. Development of the proposed navigation system is given in sec. 3. Section 4 presents flight test results and concluding remarks are given in sec. 5.

2. Fault Detection and Isolation Algorithm

2.1 Fault detection and isolation algorithm for integration Kalman filter

The error model of the Kalman filter is of the order of 15. The 15 state comprises 3 position errors, 3 velocity errors, 3 attitude errors, 3 gyroscope errors and 3 accelerometer errors. The position, velocity, and attitude data from ADGPS receiver are utilized as measurements for the Kalman filter. Details of the error model and the measurement equation are described in another paper (Oh et al., 2001). Generally the major error source of IMU is bias (Titterton and Weston, 1997). In the proposed integrated navigation system, the IMU errors are modeled as random biases. However, the low grade IMU contains other significant error sources such as drift, scale factor error, and misalignment (Titterton and

Weston, 1997). When the Kalman filter adopts such a simplified model, the uncertainty of the error model is increased and the quality of the ADGPS data is much more important. Therefore, in order to guarantee the reliability and accuracy of the navigation system, an FDI algorithm should be considered to detect and reject the anomalous ADGPS data from measurements.

Figure 2 illustrates the FDI algorithm for the proposed ADGPS/INS integration system. First, hard failures of the INS are checked in the BIT result of the IMU. The FDI algorithm consists of 4 parts; ① residual generation, ② test statistic generation, ③ fault detection, and ④ fault isolation.

The part ① generates residuals from the ADGPS output and the INS output. If the system has no fault, the residual vector $\boldsymbol{\gamma}_k$ is assumed to be white Gaussian vector with zero mean and covariance $\mathbf{V}_k$ as follows (Maybeck, 1979).

$$\boldsymbol{\gamma}_k = \mathbf{z}_k - \mathbf{H}_k\mathbf{x}_k \sim N(0, \mathbf{V}_k) \tag{1}$$

where $\mathbf{x}_k$ and $\mathbf{z}_k$ are the state vector and the measurement vector, respectively; $\mathbf{H}_k$ is the measurement matrix.

The part ② generates a chi-square distributed test statistic with the residuals in the part ① and the residual covariance matrix from the Kalman filter.

$$\mathbf{V}_k = \mathbf{H}_k\mathbf{P}_k\mathbf{H}_k^T + \mathbf{R}_k \tag{2}$$

$$l_k = \sum_{i=k-N+1}^{k} \boldsymbol{\gamma}_i^T \mathbf{V}_i^{-1} \boldsymbol{\gamma}_i \sim \chi^2_{Np} \tag{3}$$

where $\mathbf{P}_k$ is the error covariance matrix and l_k is the chi-square distributed test statistic with $N \cdot p$ degrees-of-freedom (DOF). The N and p denote the window size and dimension of the residual vector, respectively. The part ③ decides whether the fault occurs or not from the following decision criterion (Da, 1994; Brumback and Srinath, 1987).

$$\begin{cases} \text{if } l_k \geq \varepsilon \text{ then there is a fault} \\ \text{if } l_k \geq \varepsilon \text{ then there is no fault} \end{cases} \tag{4}$$

where ε is the decision threshold.

For the chi-square distributed test statistic, the decision threshold can be determined from the DOF of test statistic and the false alarm rate in the chi-square distribution table. If the residual vector is not white Gaussian, the test statistic is not a completely chi-square distributed random variable (Grewal et al., 2001). In this case, the decision threshold should be adjusted through a trial and error approach. The FDI algorithm is separately applied to the position, velocity, and attitude measurements. The detection result of part ③ is transferred to the part ④. The part ④ performs the fault isolation. In order to prevent performance degradation due to faulty GPS data, the integration Kalman filter does not use that data.

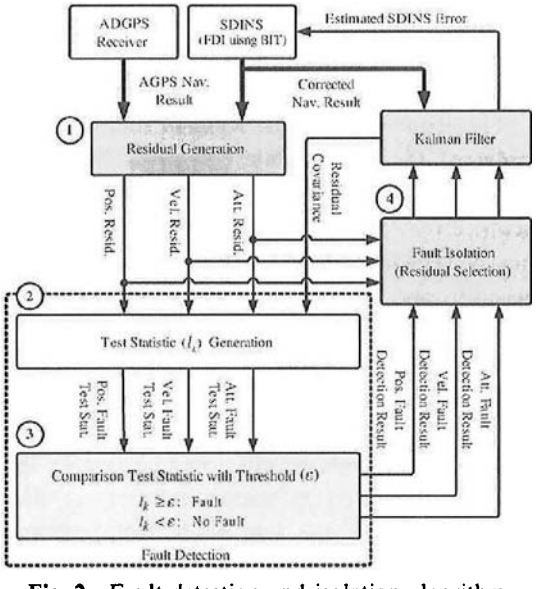

Fig. 2 Fault detection and isolation algorithm

2.2 Selection of Q, R Value and FDI Algorithm

The integration Kalman filter performance can be adjusted through the $\mathbf{Q}$ (process noise covariance matrix) and $\mathbf{R}$ (measurement noise covariance matrix) value tuning (Maybeck, 1979). The $\mathbf{Q}$ and $\mathbf{R}$ denote the uncertainty of the INS error model and the measurement, respectively. A small $\mathbf{Q}$ value implies an accurate INS error model, and the measurement is lightly weighted. Similarly, a small $\mathbf{R}$ value implies an accurate

measurement (Maybeck 1979). When the **Q** value is large, the output of the integrated navigation system will closely follow the ADGPS outputs and the residual and test statistic becomes a small value.

As mentioned previously, the integrated Kalman filter performs only the time propagation when anomalous GPS measurements are detected. During this period if an excessively large **Q** value is given, the test statistic becomes too small and the FDI algorithm cannot detect the fault. Conversely, if an excessively small **Q** value is given, the test statistic becomes a large quantity and false alarms occur too often.

3. ADGPS/INS Integrated Navigation System

3.1 Hardware description

Figure 3 describes the hardware structure of the proposed ADGPS/INS integrated navigation system. The hardware comprises an integrated navigation package (INP) and a commercial IMU. The INP includes an ADGPS receiver and a navigation computer unit (NCU) in single case. The ADGPS receiver has three GPS signal processing parts for real-time attitude determination. The RF front end and correlator of the signal processing part is designed with GP2010 and GP2021 chipset (manufactured by Zarlink Semiconductor). The NCU executes the integration algorithm and exchanges data with other subsystem in the UAV. EEPROM is used for firmware and SRAM is used for real-time data storage. The NCU contains synchronous/asynchronous serial interfaces such as UART, SDLC, and ARINC 429 to exchange data with the ADGPS receiver, IMU, and FCC in the UAV. The SDLC and ARINC 429 interface are designed with Z16C30 (manufactured by Zilog, Inc.) and DD-00429 (manufactured by Data Device Corporation) chipset, respectively. Any commercial IMU can be applied in the proposed integrated navigation system hardware if it gives output data through the standard serial interface such as RS-232 or RS-422.

3.2 Software description

The navigation system should process the data in real-time and it can be easily modified and

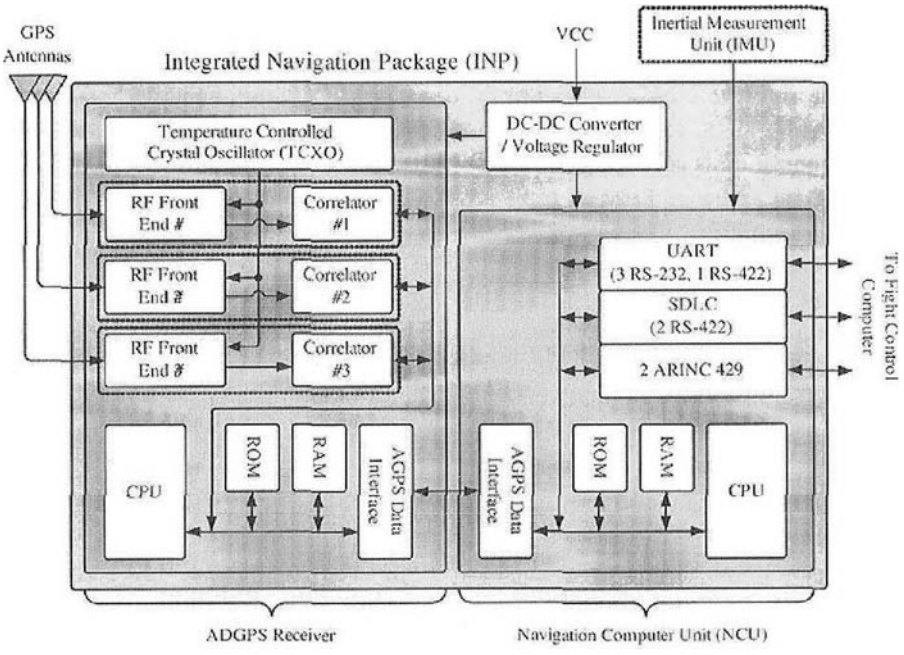

Fig. 3 Hardware scheme of proposed integrated navigation system

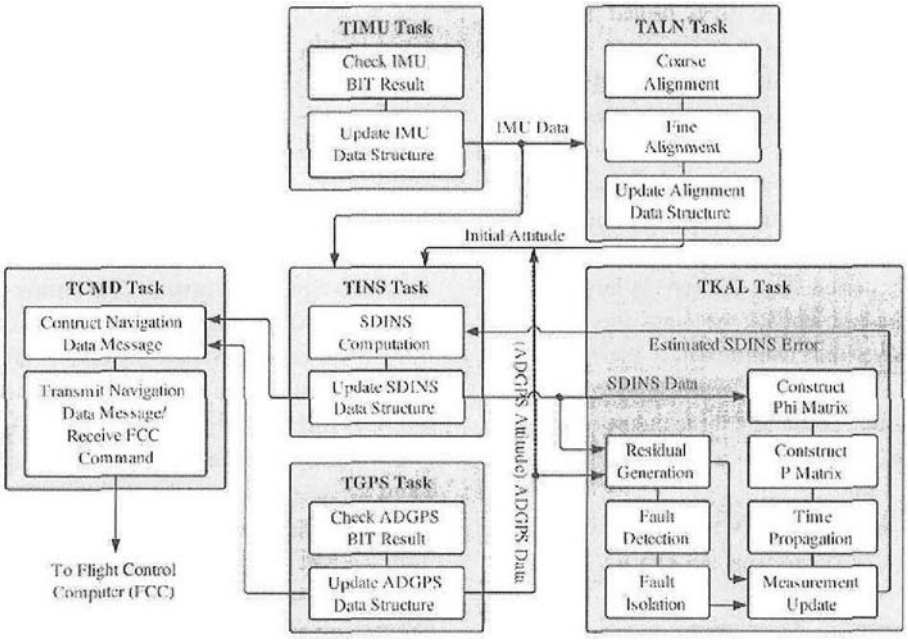

Fig. 4 Implemented real-time software based on multitasking structure

reconfigured according to the specification of the UAV (Mathes et al., 2003 ; Newport, 1994). For this purpose, a real-time software for the proposed navigation system is designed and developed on the multi-tasking environment, a commercial real-time operating system (RTOS) (manufactured by WindRiver Inc., pSOSystem).

Figure 4 shows the real-time software structure in the NCU. The software consists of 6 tasks ; TIMU, TGPS, TALN, TINS, TKAL, and TCMD task. Task synchronization is accomplished using the semaphores. Data exchange between tasks is performed through global structure variables and message queues.

The TIMU task updates members of the IMU related data structure and decides whether there is a fault in the IMU or not. The TGPS task updates the ADGPS related information in the ADGPS related data structure and monitors the hardware failure in the ADGPS receiver.

The TALN task runs the initial alignment process. When the tactical or higher grade IMU is used in the navigation system, the gyrocompass method in the TALN task provides initial attitude of the vehicle. If low grade IMU is used, the initial alignment result is replaced with the attitude output provided by the ADGPS receiver.

The TINS task runs the strapdown inertial navigation algorithm. The attitude computation in the algorithm adopts the quaternion update method (Titterton and Weston, 1997). The position and velocity are computed in the local-level frame. Then these values are transformed into those in the other coordinate system.

The TKAL task runs the integration Kalman filter and the FDI algorithm. The extended Kalman filter (EKF) is implemented in feedback configuration. The error covariance matrix is updated using the Upper-triangular Diagonal (UD) factorization method for numerical stability (Maybeck, 1979). The FDI algorithm described in sec. 2 is implemented as a module in the TKAL task.

The TCMD task manages commands and messages to/from the FCC.

4. Flight test

In order to evaluate the performance of the proposed ADGPS/INS integrated navigation system, flight tests were conducted, which were designed to include the different types of maneuver

for simulation of the UAV motion. Tactical and automotive grades IMU were used for the flight test to demonstrate the effectiveness of the proposed integration scheme with the FDI algorithm. The flight test data were collected by a data acquisition (DAQ) system and analyzed in the laboratory after the flight tests.

4.1 Experiment setup

The flight test vehicle was a single-engined, four-seater small aircraft developed by the KARI, Korea. Figure 5 shows the photograph of the test aircraft. Table 1 describes the specification of the aircraft.

Figure 6 illustrates a plan view of the GPS antenna installation. Three aircraft GPS antennas were mounted on the roof of the aircraft for attitude determination. Table 2 shows the specification of the GPS antenna.

Figure 7 shows the installation of IMUs. The tactical grade ring laser gyro (RLG) IMU was installed on the floor of the aircraft using an aluminum mount and the automotive grade micro

Table 1 Specification of flight test aircraft

	Description
Seating Capacity	4
Overall Length (m)	10.4
Max. Take-off Weight (ton)	1.2
Max. Range Cruse (km)	1,850
Cruising Speed (km/h)	280
Operating Altitude (km)	2.4

Fig. 5 Photograph of small aircraft for flight test

Table 2 Specification of GPS antenna

		Description
Manufacturer		Sensor Systems Inc.
Model		S67-1575-49
Center Frequency (MHz)		1575.42
Gain	Antenna (dBic)	3 (@ Zenith, Typical)
	Preamplifier (dB)	40
Impedance (Ω)		50
VSWR		2.0
Noise Figure (dB)		2.8
Vibration (G's)		10
Altitude (ft)		55,000

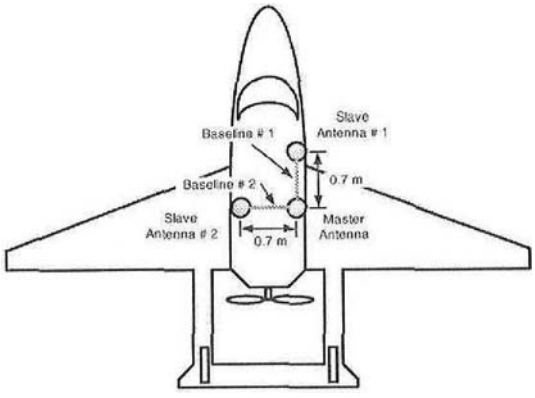

Fig. 6 Plan view of GPS antenna installation

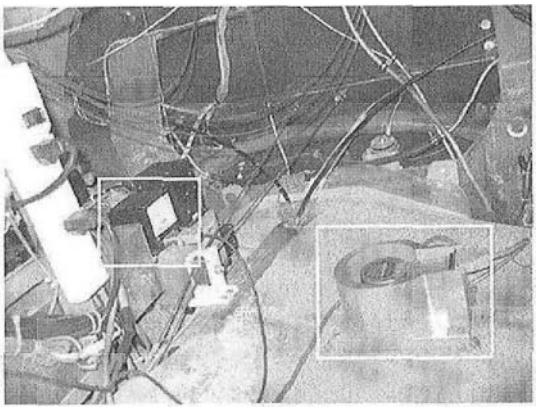

Fig. 7 Installation of IMU
(Left : MEMS IMU, Right : RLG IMU)

Table 3 Specification of IMUs

	Description	
Manufacturer	Honeywell	Crossbow
Model	HG1700AE11	DMU-H6X
Grade	Tactical	Automotive
Gyro Type	Ring Laser	MEMS
Gyro Bias (°/h)	1.0	3600
Gyro Noise (°/$\sqrt{h}$)	0.125	2.250
Accel Bias (mg)	1.0	10.0
Accel. Noise (m/s/$\sqrt{h}$)	0.024	0.150
Interface	SDLC (RS-422)	UART (RS-232)
Output Rate (Hz)	100	100
Size (mm)	93.98 dia×73.66 ht	76.2×95.3×81.3
Power (W)	<8	<3

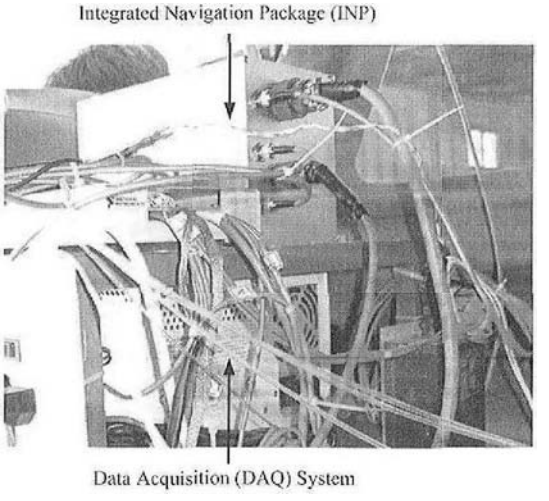

Fig. 8 Installation of integrated navigation package and data acquisition system

electro-mechanical system (MEMS) IMU was mounted on the longitudinal axis of the fuselage. The specification of each IMU is described in Table 3.

The installation of INP and DAQ system is shown in Fig. 8. The National Instruments DAQ system records not only the in-flight navigation data from the ADGPS/INS integrated navigation system, but also the raw data of the each IMU and other sensors in the test aircraft for the off-line data processing and performance analysis.

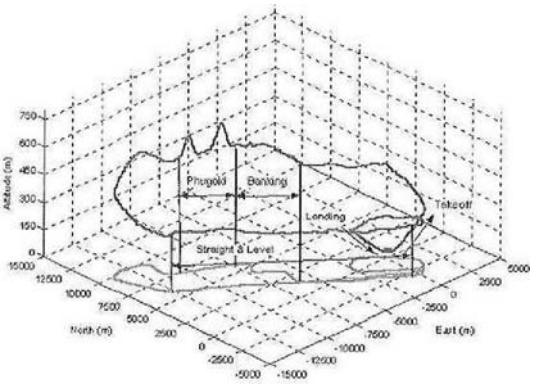

Fig. 9 Flight test path

4.2 Flight test result

The test aircraft conducted several types of aneuver for the performance evaluation. The flight test path is illustrated in Fig. 9. The total flight distance was 55.5 km and flight time 23 minutes. During the test, the maximum ground speed and acceleration reached 252 km/h and 2 G, respectively. After takeoff, the test aircraft goes up to 620 m altitude for 100 seconds with 10 degrees climb angle to enter the maneuver area. In the maneuver area, it performs 2 sets of motion, banking and phugoid. During the phugoid motion, total elevation change was approximately 150 m. Subsequently, the test aircraft descends to 300 m altitude and conducts the straight and level

Table 4 *Flight test profile*

Profile No.	Type of Maneuver	GPS Time (Duration)
1	±20 and ±50 deg Banking	111,329~111,423 s (94 s)
2	+20/−10 and +15/−10 deg Phugoid	111,424~111,499 s (75 s)
3	Straight and Level	111,662~111,899 s (237 s)

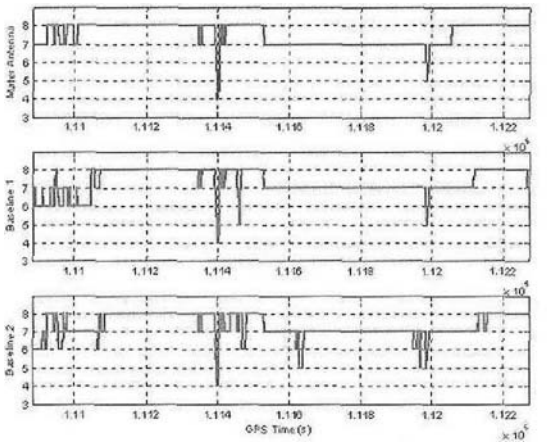

Fig. 10 Number of satellites in view during flight test

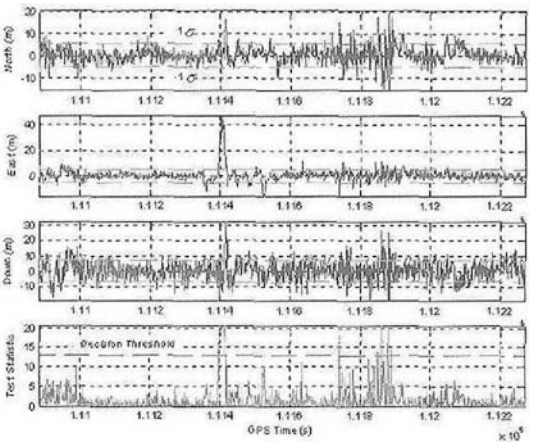

Fig. 11 Position differences between ADGPS receiver and ADGPS/RLG IMU

flight with average 217 km/h ground speed for 240 seconds toward the vicinity of airfield. Finally, it performs 180 degrees turning to approach the runway and lands from the opposite direction of takeoff. The profile is summarized in Table 4.

Figure 10 shows number of satellite in view at the master antenna and each baseline. It can be seen that satellite visibility was good; the maximum number of satellite was 8. On the runway, number of visible satellite was changed frequently due to the signal blockage by the hangar. After takeoff, the number of satellite in view was 8. During the profile 1, the number of common satellite by baselines drops to 4. That changed into 7 during the profile 3. The number of common satellite decreases temporarily to 5 when the test aircraft conducts the banked turn to approach the runway. That recovered rapidly to 8 during the landing.

Since a highly accurate navigation system, which can be regarded as a reference navigation system for performance evaluation, could not be installed in the test aircraft, the proposed integrated navigation system was evaluated by observing navigation output differences between the ADGPS receiver and the proposed ADGPS/INS integrated navigation system and the error covariance values of the integration Kalman filter and comparing the roll and pitch output with those of a vertical gyroscope. The vertical gy-

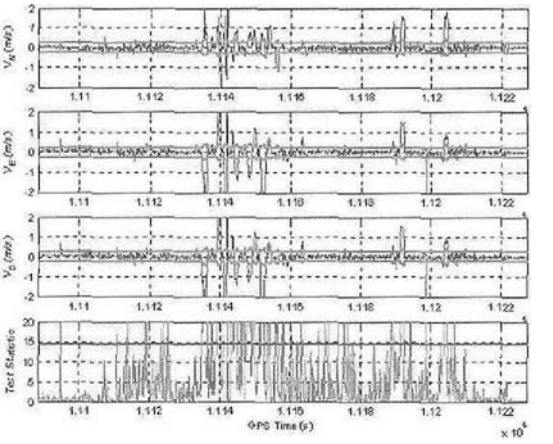

Fig. 12 Velocity differences between ADGPS receiver and ADGPS/RLG IMU

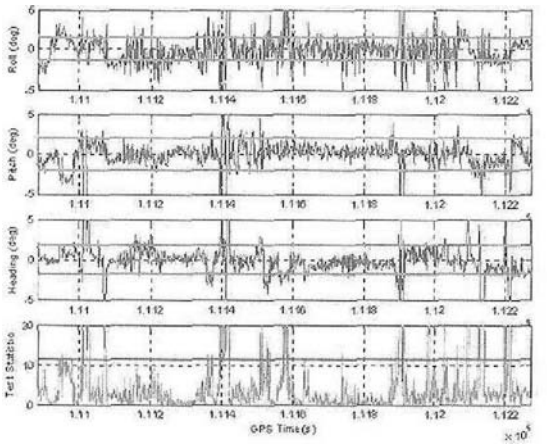

Fig. 13 Attitude differences between ADGPS receiver and ADGPS/RLG IMU

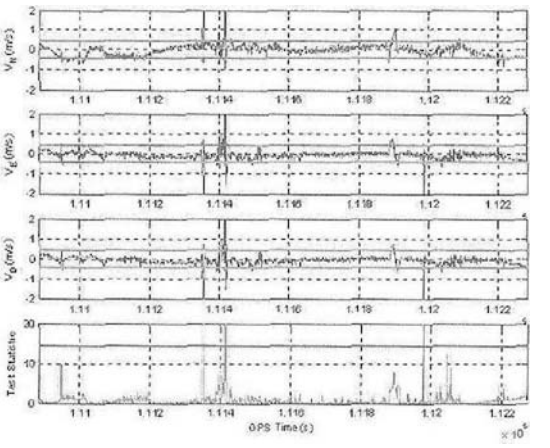

Fig. 15 Velocity differences between ADGPS receiver and ADGPS/MEMS IMU

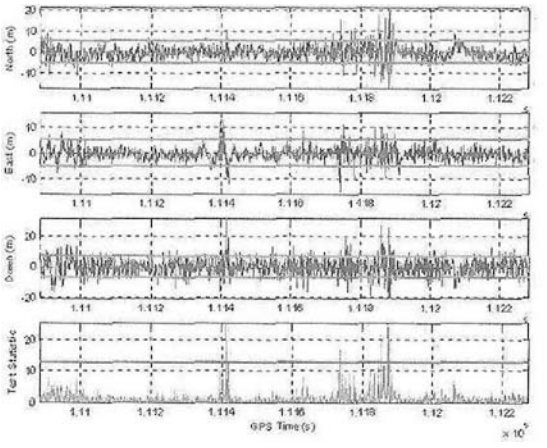

Fig. 14 Position differences between ADGPS receiver and ADGPS/MEMS IMU

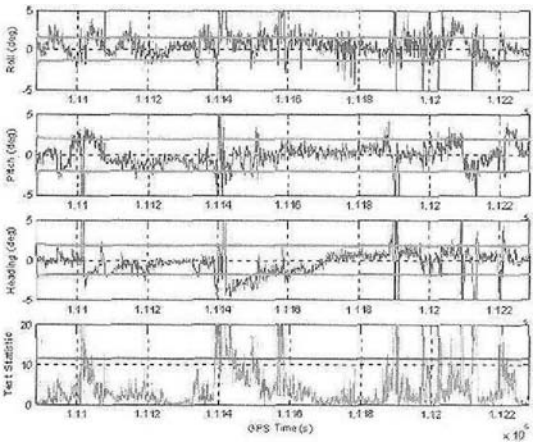

Fig. 16 Attitude differences between ADGPS receiver and ADGPS/MEMS IMU

roscope used in the evaluation was the Aeronetic RVG-801E vertical gyroscope which provides the roll and pitch angle at 50 Hz with the ± 0.5 degrees RMS error.

The navigation output differences between the ADGPS receiver and ADGPS/INS integrated navigation system are shown from Fig. 15 and 16. In each figure, first three subplots show the difference of navigation result and fourth subplot shows the test statistic used for the FDI. The bold lines in each subplot denote the standard deviation of the difference of navigation result and decision threshold, respectively.

When the FDI was implemented, different decision thresholds were chosen for all of the measurement variables in order to take account of the quality of the GPS measurements. The window size N was chosen as 1 and the false alarm rate for position, velocity, and attitude measurements are selected as 0.5%, 0.25%, and 1.0%, respectively. These alarm rates were firstly chosen after the quality of the GPS measurement output was checked and adjusted through a trail and error method.

Table 5 gives detected number of fault of the navigation system when the FDI algorithm is applied. The ADGPS/MEMS IMU integration has relatively smaller test statistic than the ADGPS/

Table 5 Number of fault detection of each ADGPS/INS integrated navigation system

	ADGPS/RLG IMU	ADGPS/MEMS IMU
Position	27	8
Velocity	187	6
Attitude	126	89

Table 6 Standard deviation of estimated navigation error of ADGPS/INS integrated navigation system

		ADGPS/RLG IMU	ADGPS/MEMS IMU
Position (m)	North	1.18	1.69
	East	1.18	1.69
	Down	1.39	1.98
Velocity (m/s)	V_N	0.13	0.35
	V_E	0.13	0.35
	V_D	0.13	0.35
Attitude (deg)	Roll	0.02	0.12
	Pitch	0.02	0.11
	Heading	0.06	0.11

RLG IMU integration since a larger **Q** value was used for lower performance IMU. For this reason, the ADGPS/MEMS IMU integration has smaller number of detected fault compared with the ADGPS/RLG IMU integration.

Table 6 shows the standard deviation of the estimated error of each navigation system. Position errors of integration systems are less than 2 m. Velocity and attitude errors of the ADGPS/RLG IMU integration system are respectively about 3 and 5 times less than those of the ADGPS/MEMS IMU, except for the heading error.

Figure 17 and 18 show some interesting parts of attitude output of the navigation systems with the output of vertical gyroscope. Figure 17 shows roll angle output during the banking motion in the profile 1. In Fig. 17, it is observed that when the aircraft conducts roll motion from -50 degrees to level the ADGPS receiver cannot provide the attitude data due to the lack of satellites in view (cf. Fig. 10). It can be noted that both of the proposed ADGPS/MEMS and RLG IMU integration system still provides attitude result even in this situation.

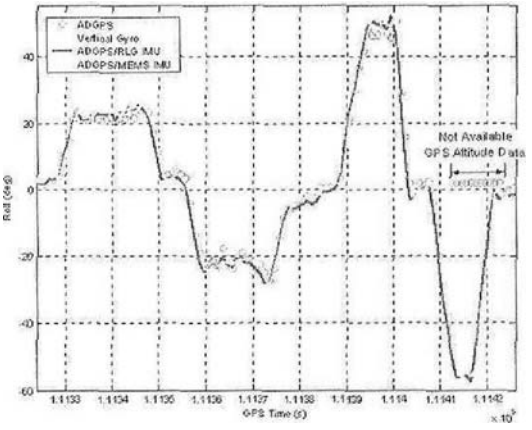

Fig. 17 ±20 and ±50 degrees banking motion in profile 1

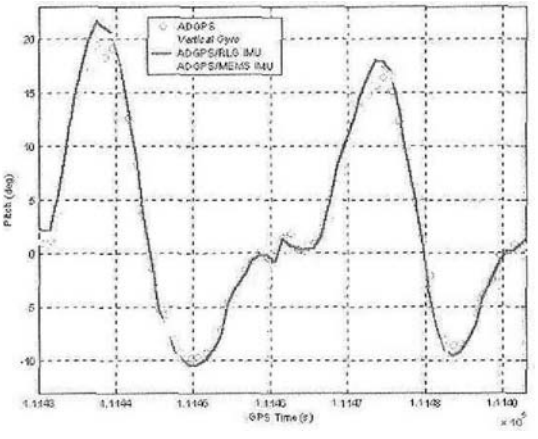

Fig. 18 +20/−10 and +15/−10 degrees phugoid motion in profile 2

The pitch angle output during the phugoid motion in the profile 2 is shown in Fig. 18. Figure 18 shows that when the test aircraft is in pitch motion from −10 degrees pitch to level the ADGPS/MEMS IMU integration gives result off approximately 3.5 degrees from that of the vertical gyroscope. It is noted that the ADGPS/RLG IMU integration outputs are almost the same as those of the vertical gyroscope.

Table 7 presents the statistical values of the attitude differences between the proposed integrated navigation systems and the vertical gy-

Table 7 Comparison of attitude result from each navigation system

		ADGPS Receiver	ADGPS/RLG IMU	ADGPS/MEMS IMU
Roll Difference (deg)	Mean	−0.53	−0.52	0.53
	STD	1.68	0.92	2.02
	Max.	4.78	2.88	6.07
Pitch Difference (deg)	Mean	−0.05	0.53	−0.40
	STD	2.19	0.96	2.30
	Max.	4.65	2.54	3.42

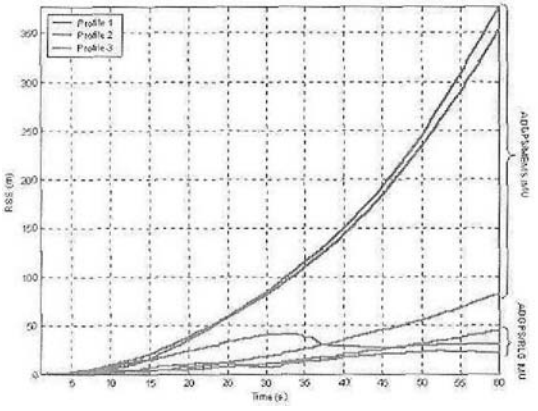

Fig. 19 Comparison of RSS position error during GPS outage in each flight profile

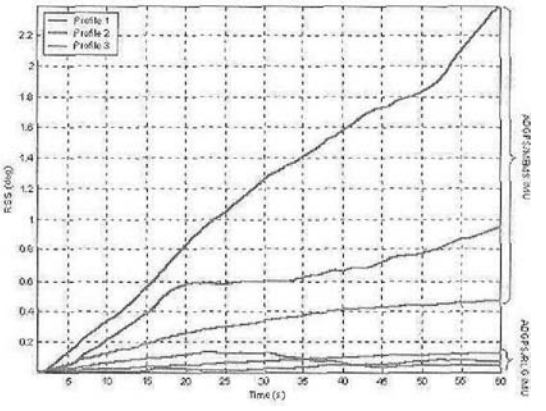

Fig. 21 Comparison of RSS attitude error during GPS outage in each flight profile

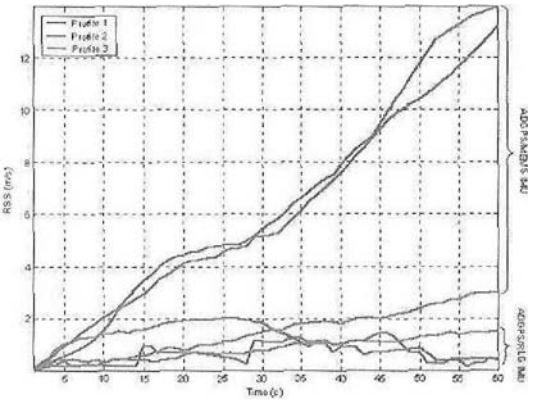

Fig. 20 Comparison of RSS velocity error during GPS outage in each flight profile

roscope during the motion in the profile 1 and 2. The cases of ADGPS receiver are excluded from the computation when the attitudes are not provided. Table 7 shows that ADGPS/MEMS IMU integration attitude performance is very close to the ADGPS receiver and the ADGPS/RLG IMU attitude performance is best among three systems.

To access coasting capability of the proposed integrated navigation system, GPS signal outage was simulated by removing GPS measurement for a given period of time. The coasting test results are given in Figs. 19~21. At the start of each flight test profile, GPS signals are lost for 60 seconds. The root-sum-square (RSS) error is calculated from the difference between the output of ADGPS receiver and each integration system.

The ADGPS/MEMS IMU integration system shows large differences in coasting capability for profiles. The RSS error is large during the phugoid motion in the profile 2 while that is small during the straight and level flight in the profile 3. The ADGPS/RLG IMU integration system gives similar results in coasting capability for all profiles.

Table 8 shows the maximum RSS errors of the coasting capability. The maximum RSS position,

Table 8 Comparison of maximum RSS error during GPS outage in each flight profile

Maximum RSS Error		ADGPS/RLG IMU	ADGPS/MEMS IMU
Profile 1	Position (m)	40.97	351.77
	Velocity (m/s)	1.97	13.16
	Attitude (deg)	0.13	0.95
Profile 2	Position (m)	23.34	376.39
	Velocity (m/s)	1.23	13.94
	Attitude (deg)	0.08	2.39
Profile 3	Position (m)	44.84	82.09
	Velocity (m/s)	1.49	3.03
	Attitude (deg)	0.12	0.47

Table 9 Comparison of coasting capability result between proposed integration system and GIGET simulation during for 60 seconds GPS outage

	Tactical Grade IMU		Automotive Grade IMU	
	ADGPS/RLG IMU	GIGET (1 deg/h Gyro Bias)	ADGPS/MEMS IMU	GIGET (100 deg/h Gyro Bias)
Position (m)	36.4	54.6	270	272
Velocity (m/s)	1.56	1.87	10.04	14.60
Attitude (deg)	0.11	0.22	1.27	3.68

velocity, and attitude error of the ADGPS/RLG IMU integration are less than 45 m, 2 m/s, and 0.14 degrees, respectively. When the MEMS IMU is used for the integration, those values are less than 377 m, 14 m/s, 2.4 degrees, respectively.

Guatier and Parkinson (2003) has carried out the coasting simulation using the GPS/INS generalized evaluation tool (GIGET) developed by Stanford University to compare the performance of integration systems using tactical (1 deg/h gyro bias) and automotive grade (100 deg/hr gyro bias) IMU with ADGPS. Table 9 gives the comparison of coasting capability result between the proposed integration systems and GIGET simulation. In this table, the coasting capability result of the proposed integration system is the mean value over all maximum RSS values of each profile. It is noted that the proposed ADGPS/INS navigation system gives better coasting capability than the GIGET simulation. Especially in the case of automotive grade IMU, the ADGPS/MEMS IMU integration provides notable coasting capability in spite of very lower performance of IMU than the GIGET simulation. When a UAV requires more reliable and accurate navigation performance even in GPS signal outage, the tactical grade IMU seems to be more suitable for the ADGPS/INS integrated navigation system.

5. Concluding Remarks

In this paper, an ADGPS/INS integrated navigation system with the FDI algorithm for a UAV has been proposed. An integration algorithm with the FDI function has been proposed to guarantee the reliability and integrity of navigation system even when the low grade IMU is utilized. The Effect of **Q** and **R** value selection on the performance of the FDI has been discussed and the real-time software and hardware scheme for integrated navigation system has been described.

In order to assess the performance of the proposed ADGPS/INS navigation system, a flight test has been performed under a couple of dy-

namic environments. A tactical and automotive grade IMUs have been used for the flight test to demonstrate the effectiveness of proposed integration scheme.

The flight test result demonstrated that the proposed navigation system provided a reliable performance against anomalous GPS data and an accurate navigation result even in the high dynamic roll and pitch maneuvers, and good coasting capability for the complete GPS signal outage.

References

Blakelock J. H., 1991, *Automatic Control of Aircraft and Missiles, 2nd edition*, John Wiley & Sons, New York.

Brenner, M., 1995, "Integrated GPS/Inertial Fault Detection Availability," *Proceedings of the ION GPS-95*, pp. 1949~1958.

Brumback, B. D. and Srinath, M. D., 1987, "A Chi-Square Test for Fault-Detection in Kalman Filters," *IEEE Transactions on Automatic Control*, Vol. AC-32, No. 6, pp. 552~554.

Cox, D. B., 1980, "Integration of GPS with Inertial Navigation Systems," reprinted in *Collected GPS Papers*, Vol. I, pp. 144~153, Institute of Navigation, Alexandria, VA.

Da, R., 1994, "Failure Detection of Dynamical Systems with the State Chi-Square Test," *Journal of Guidance, Control, and Dynamics*, Vol. 17, No. 2, pp. 271~277.

Diesel, J. and King, J., 1995, "Integration of Navigation System for Fault Detection, Exclusion, and Integrity Determination-Without WASS," *Proceedings of the ION GPS-95*, pp. 683~692.

Gautier, J. D. and Parkinson, B. W., 2003, "Using the GPS/INS Generalized Evaluation Tool (GIGET) for the Comparison of Loosely Coupled, Tightly Coupled and Ultra-Tightly Coupled Integrated Navigation Systems," *Proceedings of the ION 59th Annual Meeting*, pp. 65~76.

Gebre-Egziabher, D., Hayward, D. R. and Powell, C. D., 1998, "A Low-Cost GPS/Inertial Attitude Heading Reference System (AHRS) for General Aviation Applications," *Proceedings of the Position Location and Navigation Symposium*, pp. 518~525.

Grewal, M. S., Weill, L. R. and Andrews, A. P., 2001, *Global Positioning Systems, Inertial Navigation, and Integration*, John Wiley & Sons, New York.

Hong, S. P., Lee, M. H., Rios, J. A. and Speyer, J. L., 2002, "Observability Analysis of INS with a GPS Multi-Antenna System," *KSME International Journal*, Vol. 16, No. 11, pp. 1367~1378.

Mathes, S., Herberg, J. and Berking, B., 2003, "Functional Scope and Generic Model of Integrated Navigation Systems," *The Journal of Navigation*, Vol. 56, pp. 153~175.

Maybeck, P. S., 1979, *Stochastic Models, Estimation and Control*, Vol. I, Academic Press, New York.

McMillan, J. C., 1994, "Sensor Integration Options for Low Cost Position & Attitude Determination," *Proceedings of the Position Location and Navigation Symposium*, pp. 453~459.

Michael A., 1988, *Unmanned Aircraft (Brassey's Air Power : Aircraft, Weapon Systems and Technology series, vol 3)*, Brassey's Defence Publishers, London.

Newport, J. R., 1994, *Avionic Systems Design*, CRC Press, Boca Ration.

Oh, S. H., Hwang, D. -H. and Lee, S. J., 2001, "An Efficient Integration Scheme for the INS and the Attitude Determination GPS Receiver," *Proceedings of the ION 57th Annual Meeting*, pp. 334~340.

Rios, J. A. and White, E., 2001, "Fusion Filter Algorithm Enhancements for a MEMS GPS/IMU," *Proceedings of the ION GPS 2001*, pp. 1382~1393.

Satz, H. S., Cox, D. B., Beard, R. L. and Landis, G. P., 1991, "GPS Inertial Attitude Estimation via Carrier Accumulated-phase Measurements," *Journal of the Institute of Navigation*, Vol. 38, No. 3, pp. 273~284.

Sukkarieh, S., Nebot, E. M. and Durrant-Whyte, H. F., 1999, "A High Integrity IMU/GPS Navigation Loop for Autonomous Land Vehicle Applications," *IEEE Transactions on Robotics and Automation*, Vol. 15, No. 3, pp. 572~578.

Tsach, S., Penn, D. and Levy, A., 2002,

"Advanced Technologies and Approaches for Next Generation UAVs," *Proceedings of ICAS 2002 Congress*, pp. 131.1~131.10.

Titterton, D. H. and Weston, J. L., 1997, *Strapdown Inertial Navigation Technology*, Peter Peregrinus Ltd., London, UK.

Wolf, R., Hein, G. W., Eissfeller, B. and Loehnert, E., 1996, "An Integrated Low Cost GPS/INS Attitude Determination and Position Location System," *Proceedings of the ION GPS-96*, pp. 975~981.